J. Fluid Mech. (1969), *vol.* 38, *part* 3, *pp.* 473–480
Printed in Great Britain

Visualization of transition

By F. X. WORTMANN
Institut für Aerodynamik und Gasdynamik der Universität Stuttgart

(Received 4 September 1968)

In an experimental study the development of transition downstream of Görtler vortices was investigated. With the tellurium method it was possible to distinguish beyond the Görtler vortices to successive instability modes. The first deforms the vortex pattern in a steady way and produces between each vortex pair boundary-layer profiles with two points of inflexion. When this has been established another instability mode starts, consisting of regular three-dimensional oscillations. By detailed flow visualization a nearly complete picture of the different flow patterns can be obtained.

Introduction

Visualization means drawing a picture of the configuration of motion for a large part of the field of flow. However, every picture contains an extraordinary number of single bits of information, and it is very difficult to combine single measurements to form a complete picture of a flow field. Therefore it seems impossible to avoid the use of dye-streak methods with their high information content.

In steady flows these methods can give an immediate picture, but must be used with care in unsteady flows. Instead of streamlines we get pathlines and streaklines, which may look completely different. The phenomenon of transition, however, is in principle unsteady. Therefore we have the problem of how to use the dye-streak methods with their high information density, to find a correct picture of the motion in the unsteady flow.

This question may be answered by numerical investigation as, for example, done by Hama (1959) for the shear flow of a half infinite jet with an oscillating perturbation flow. Figure 1 shows as a newer result the difference between the actual velocity profile and the line connecting the ends of many pathlines starting at the same time. The lower part shows the same with another starting time and phase. As long as the time between the start and the observation is only a fraction of the period of oscillation the difference of the velocity profiles is small enough to allow the use of the tellurium method (Wortmann 1953) or the bubble method (Clutter & Smith 1961) with acceptable accuracy. In a similar manner it is possible to find the direction and the relative amplitude of an unsteady transverse velocity from streaklines if one confines the observation to the vicinity of the starting point of the streaklines.

In the following both possibilities are used to investigate and to find a complete picture of the pattern of motion due to higher degrees of instability downstream of Görtler vortices.

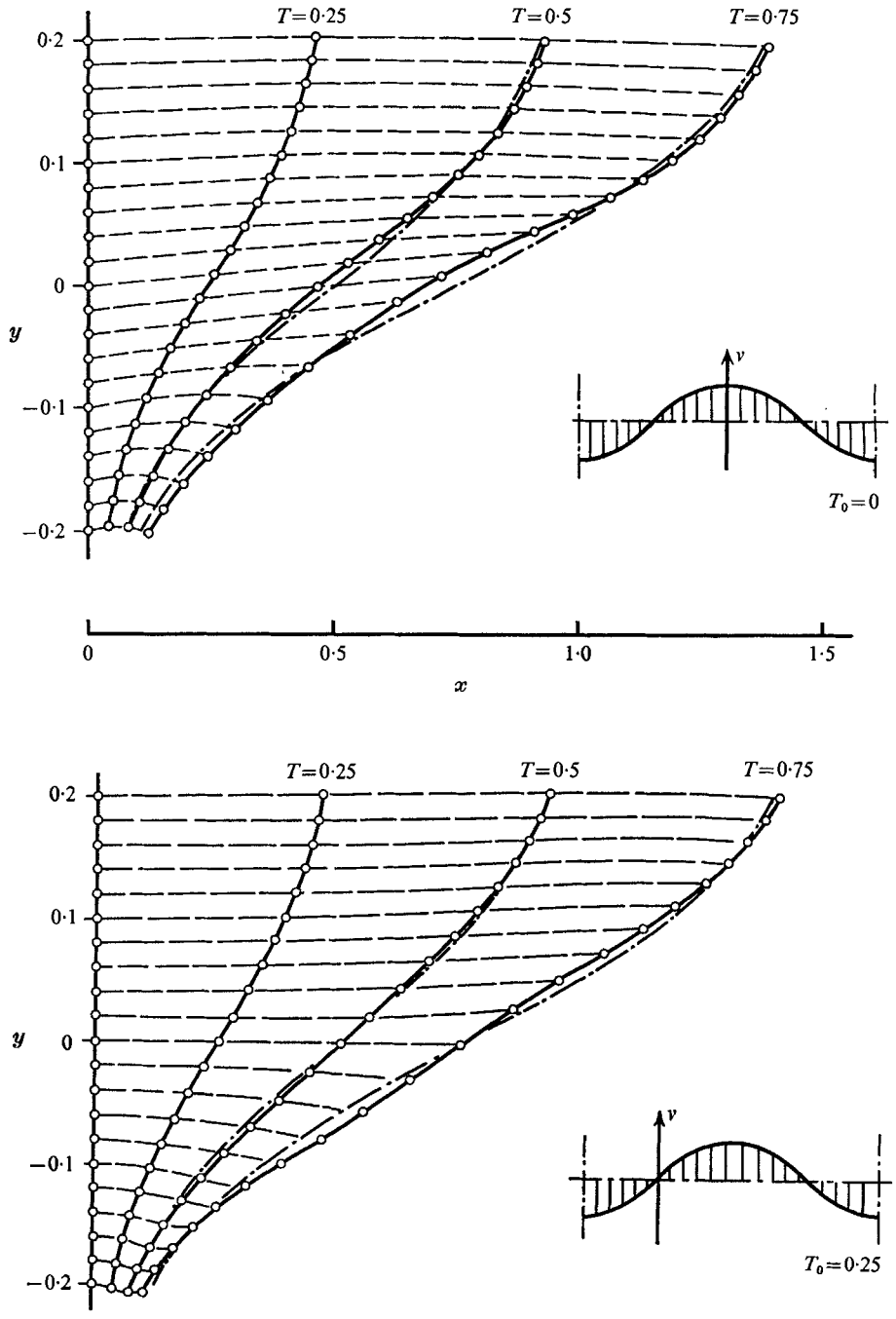

FIGURE 1. Velocity profiles and 'tellurium profiles' in the shear flow of a half infinite jet with an oscillating perturbation flow. $T = 1$ = oscillating time, $X = 1$ = wavelength. T_0 = starting time of the marked fluid particles. — — —, pathlines; —·—·—, velocity profile; —o—o—, tellurium profile. v = oscillation velocity in y direction.

Experimental arrangement

In the following experiments the same water tunnel was used as described in a previous investigation of Görtler vortices (Wortmann 1964). The test section with a length of 5 m has transparent top and side walls. The top and bottom walls are curved with a radius r of 20 m. The usual speed U_∞ of flow is 10 cm/sec. The thickness of the boundary layer three metres behind the contraction cone is 25 mm (1 inch). Therefore in this region we have a Reynolds number Re_{δ^*} of approximately 700 and a Görtler parameter

$$G = \frac{U_\infty \theta}{\nu} \sqrt{\left(\frac{\theta}{r}\right)} \approx 3,$$

where δ^* and θ are the displacement and momentum thickness respectively and ν is the kinematic viscosity.

Görtler vortices

Under the conditions just mentioned, due to a primary instability, Görtler vortices develop on the concave top wall. Figure 2 shows the pattern of motion of such vortices: at the same time we observe that a film of colour at the wall is transported into the dividing interfaces between the vortices. In figure 3, plate 1,

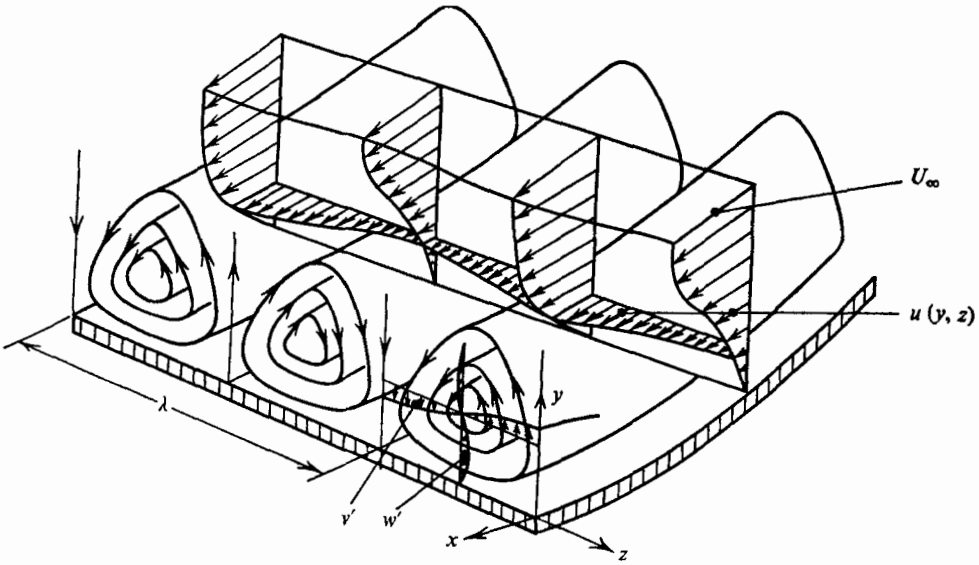

FIGURE 2. Flow pattern of Görtler vortices.

we see the test section and the contraction cone from above. In the latter a number of small perturbation wings induce vortices into the boundary layer on the top wall. The film of colour starting in the same region at the top of the figure has concentrated on the regularly spaced interfaces which is evidence of the existence of streamwise vortices.

Further downstream the vortices show a characteristic oscillation motion, which becomes turbulent a few wavelengths downstream.

During the investigation of this oscillation it came as a surprise that this motion is not due to a second-order, but a third-order instability.

Secondary instability

Before the streamwise vortices start oscillating the boundary layer is changed in a characteristic manner due to a second-order instability. If we photograph the velocity distribution in spanwise direction for several wall distances as in figure 4, plate 2, we observe that at first the peaks and valleys move slightly in spanwise direction. Figure 5 shows this move distinctly and gives in the lower

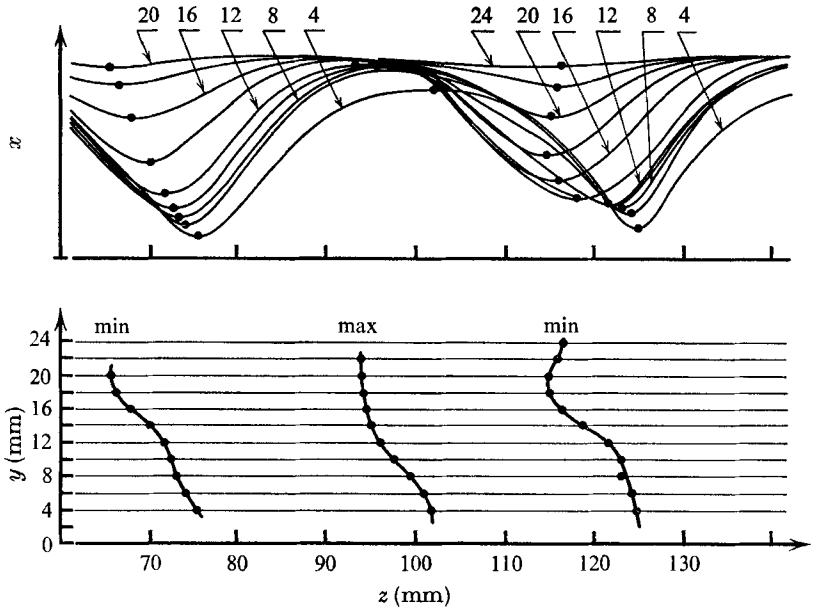

FIGURE 5. The same velocity distributions as in figure 4. The lower part shows the position of the interfaces.

part the new shapes of the interfaces, which are now no longer perpendicular to the wall. In figure 6 the results of this deformation are more striking: on one side of the oblique interfaces, corresponding to the valley, there originate boundary-layer profiles with two reversals. Figure 7, plate 3, shows a typical example. Other investigators have found these profiles to be highly instable and the immediate predecessors of turbulent 'spikes'. Here they originate in a completely steady manner. Figure 8 gives a perspective impression of the flow pattern corresponding to the second-order instability. However, the axes of the vortices remain somewhat undefined.

The onset of the second-order instability depends on the Reynolds number on one hand and on the intensity of the primary vortices on the other hand, the

latter being related to the ratio of the velocities in the peaks and valleys. In the present case with a velocity ratio of nearly 0·25 the secondary instability starts above $Re_{\delta^*} > 700$ or $G > 3{\cdot}0$.

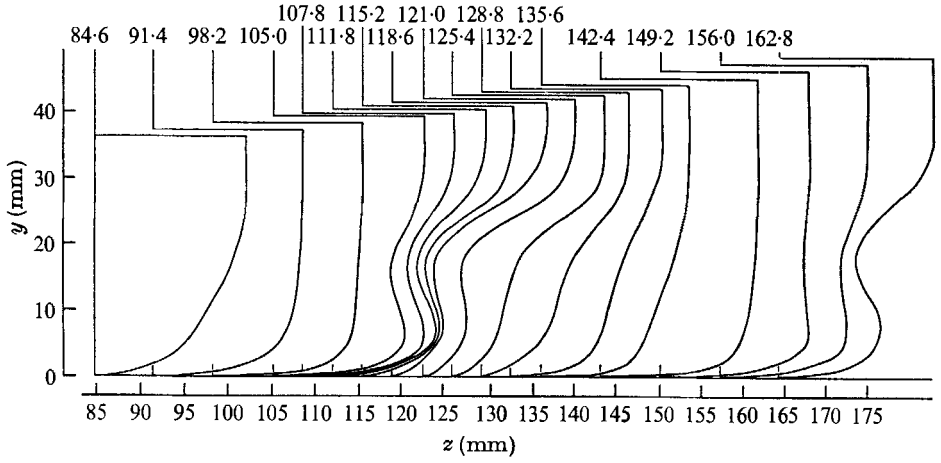

FIGURE 6. Boundary-layer profiles for several spanwise stations, when the second-order instability deforms the Görtler vortices.

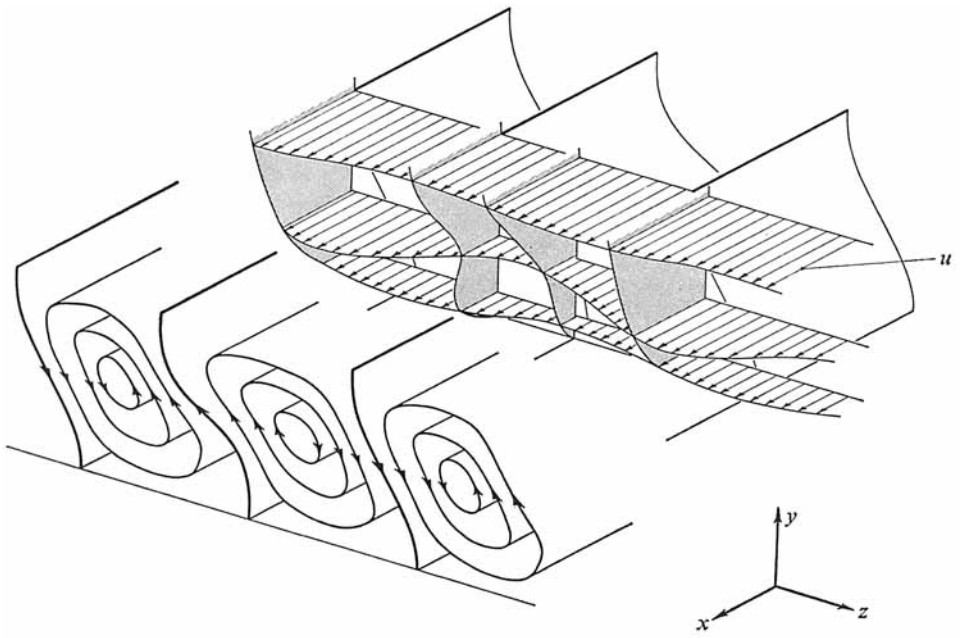

FIGURE 8. Flow pattern corresponding to the second-order instability.

The symmetry of a pair of Görtler vortices is lost due to this instability and replaced by a periodic sequence of unsymmetrical pairs of vortices. It could be imagined that the change in pattern of the streamwise vortices is caused by secondary streamwise vortices with spanwise distances double those of the Görtler vortices.

The question arises, which quality defines the sense of direction of asymmetry. In the investigation of eleven pairs of vortices it was observed, that in the right half of the tunnel the boundary-layer profiles with two reversals were to the left of the valleys and *vice versa* in the left half of the tunnel. Evidently the slight divergence of the flow at the top, which is caused by the slit suction on the corner and the secondary flow at the side walls, fixes the asymmetry. It may be pointed out that the divergence at the top wall is extremely small and not responsible for the oblique interfaces. A small reduction of the tunnel velocity or the intensity of the primary Görtler vortices restores these vortices with exactly perpendicular interfaces.

Instability of third order

To investigate the oscillation downstream of the second-order instability another single perturbation wing of dimensions 4×6 mm is located at the top wall nearly 1 m upstream of the point of observation. It rotates periodically by ± 6 degrees about an axis perpendicular to the wall and is driven by the timer, which also controls the tellurium, the camera and the flash light. The spanwise

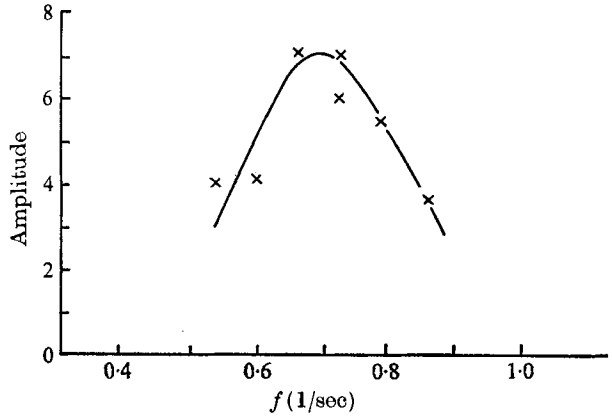

FIGURE 9. The amplitude of the oscillation as a function of the disturbing wing frequency.

position of this wing is 120 mm off the top centreline in the valley of a vortex pair, which possesses a slightly higher instability due to a little larger perturbation wing in the cone. In this way it is possible to trigger the oscillation at first in the selected vortex pair. The oscillation spreads out to the other vortex pairs on both sides, but with smaller amplitudes. In the region of observation therefore the amplitude of oscillation is not constant, neither downstream nor spanwise, but it is assumed that these gradients have no significant influence on the flow pattern. Figure 9 demonstrates that the amplitude of the oscillation has a maximum at 0·8 cycles per sec. The wavelength of the oscillation was determined by observing the phase difference between a fixed and a movable streakline probe giving a phase velocity of approximately 85 % of the outside velocity.

Figure 10 gives the results of a large number of measurements and shows the perturbation velocity u' for three wall distances and two phases dependent on

the spanwise station. There is a phase reversal at the same stations where the valley interface is located. Therefore this interface is at the same time a nodal surface of the oscillatory movement. Due to the oblique position of the interface there are stations in the vicinity of the double reversal profiles at which there are

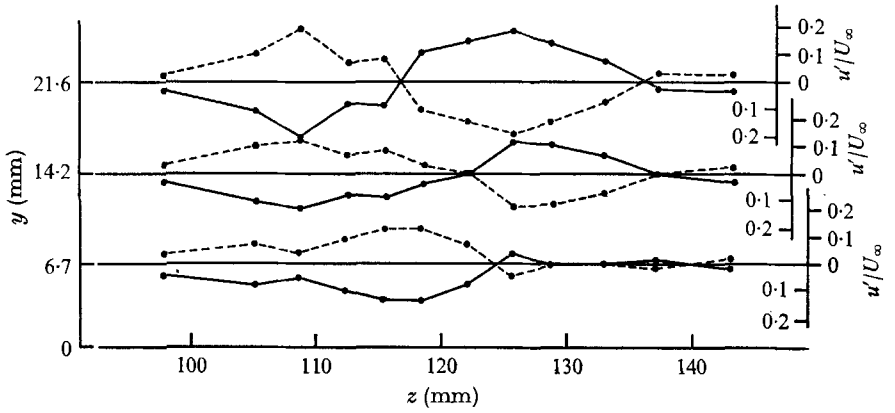

FIGURE 10. The perturbation velocity u'/U_∞ for three wall distances and two phases and several spanwise stations. — — —, $\phi = 0°$; ——, $\phi = 180°$.

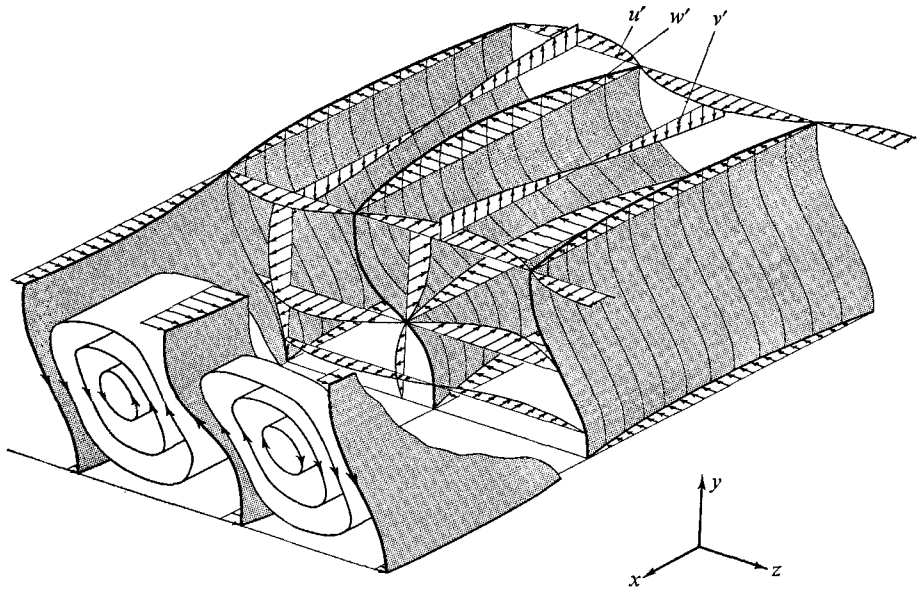

FIGURE 12. Flow pattern of the oscillating motion corresponding to the third-order instability. The steady basic flow is suppressed.

also phase reversals in the y direction. This is clearly demonstrated in figure 11, plate 4. The photograph shows the tellurium probe with two tellurium wires spaced by $\Delta z = 30{\cdot}6$ mm. The front wire at $z = 120$ mm cuts through the interface, whereas the second wire is completely contained between two interfaces. The photograph was taken twice, once at phase 0° and once at 180°, as can be seen from the streakline in the lower part of the figure. The two negatives were copied together.

The following can be said about the cross-velocities: the spanwise component w' has a maximum at the valley and the phase position is within a half wavelength the same for all y and z stations. However the v' component changes its phase from one side of the interface to the other.

Now we are in a position to draw the three-dimensional picture of the oscillation. This was attempted in figure 12. To simplify and perhaps clarify the picture the steady components of the flow are completely suppressed.

Outlook

The work presented here describes three stages in the development of transition for the special case of a boundary layer containing only streamwise vortices and may be of intrinsic interest. However, the significant details of this process may also be found in the more general case of transition at a flat plate, with certain modifications. Should this supposition prove correct, the example of flow investigated here would achieve further importance: it could be a model which simplifies access by experiments and perhaps also by theory to the higher instability modes of transition.

The author would like to express his thanks to Dipl.-Ing. M. Strunz for his continuous help in performing this work.

REFERENCES

CLUTTER, D. W. & SMITH, A. M. O. 1961 *Aerospace Engng*, **20**, 24.
HAMA, F. R. 1959 *Phys. Fluids*, **2**, 664.
WORTMANN, F. X. 1953 *Z. angew. Phys.* **5**, 201.
WORTMANN, F. X. 1964 *Proceed. XI. Int. Congr. Appl. Mech. Munich*, p. 815.

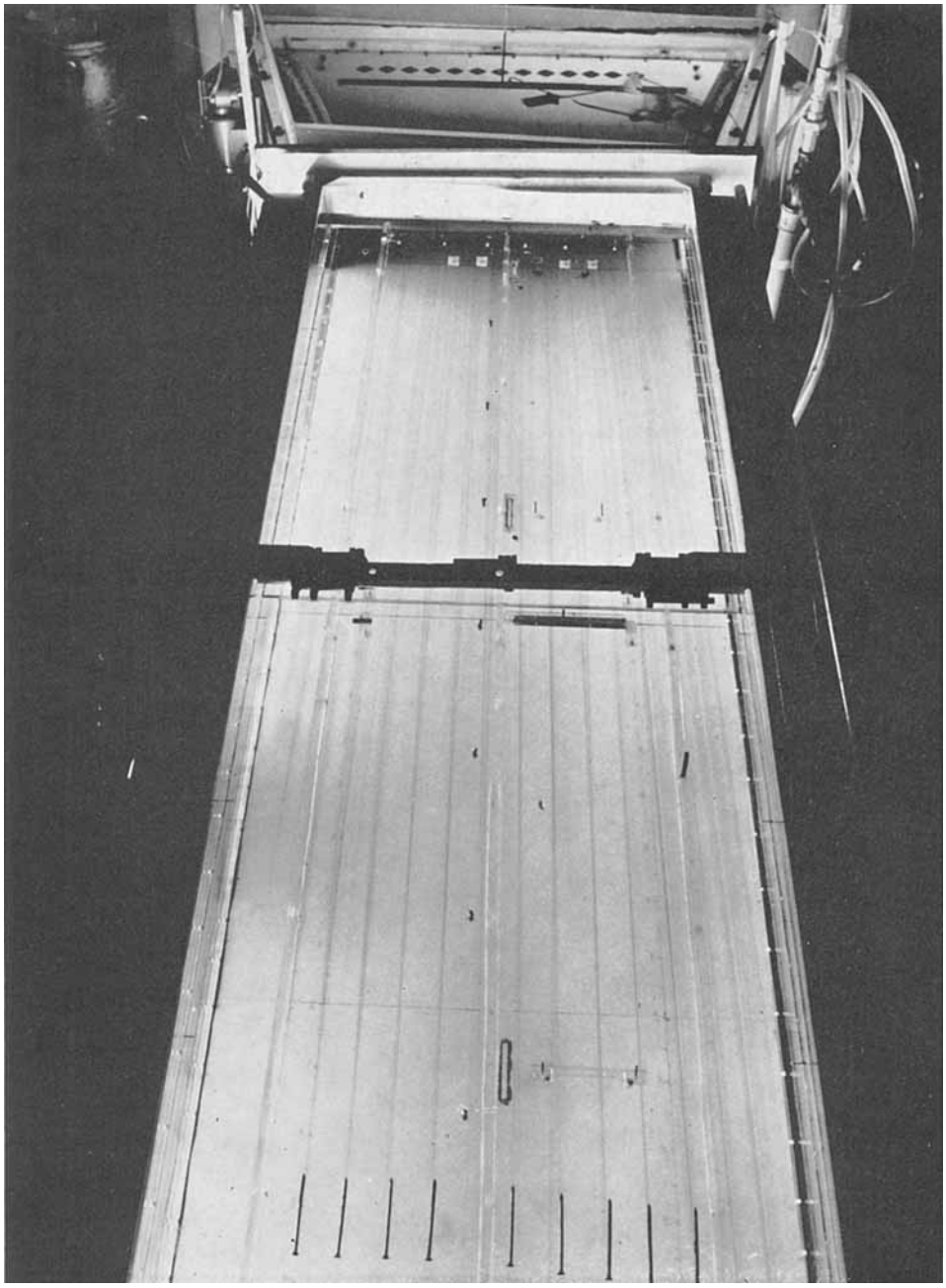

FIGURE 3. The transparent concave top wall of the test section from above. The colour film at the wall is transported into the colour streaks, which develop in the lower part of the figure by Görtler vortices.

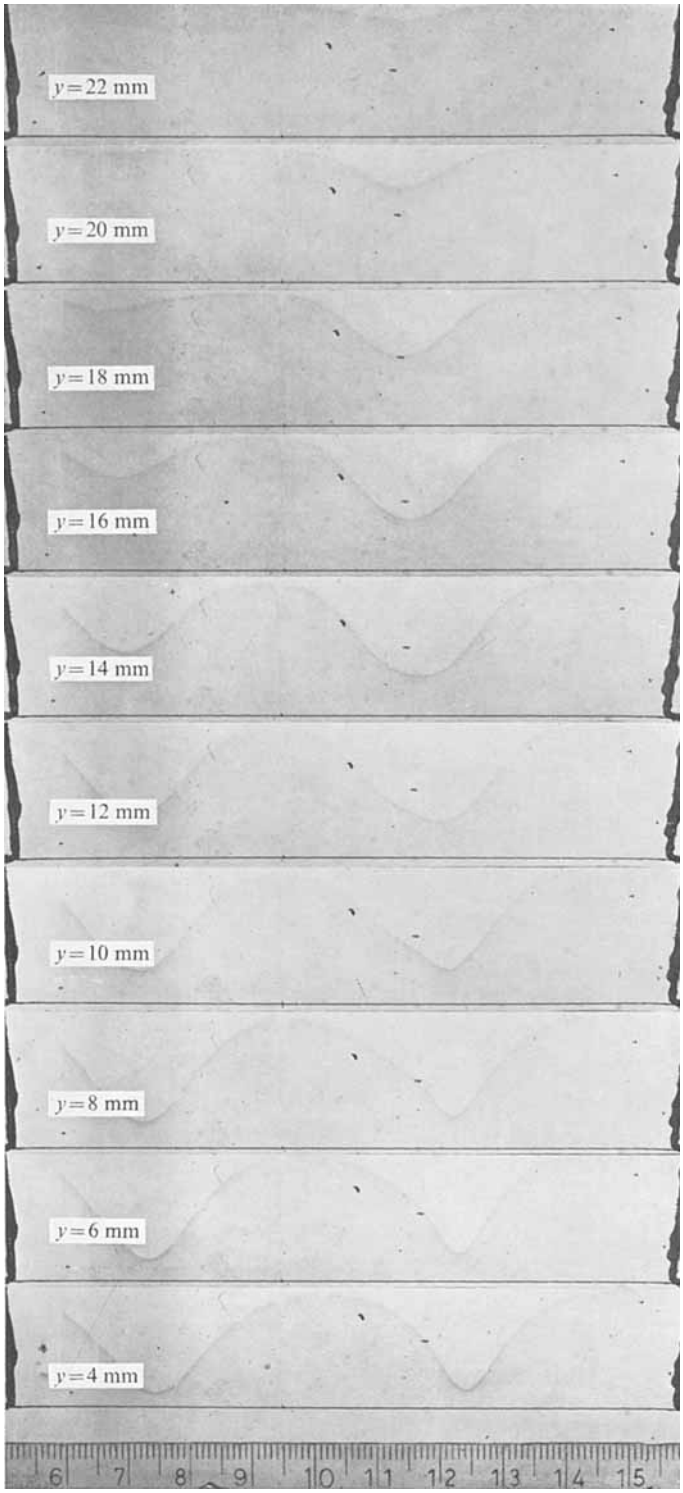

FIGURE 4. Velocity distributions at several wall distances with deformed Görtler vortices.

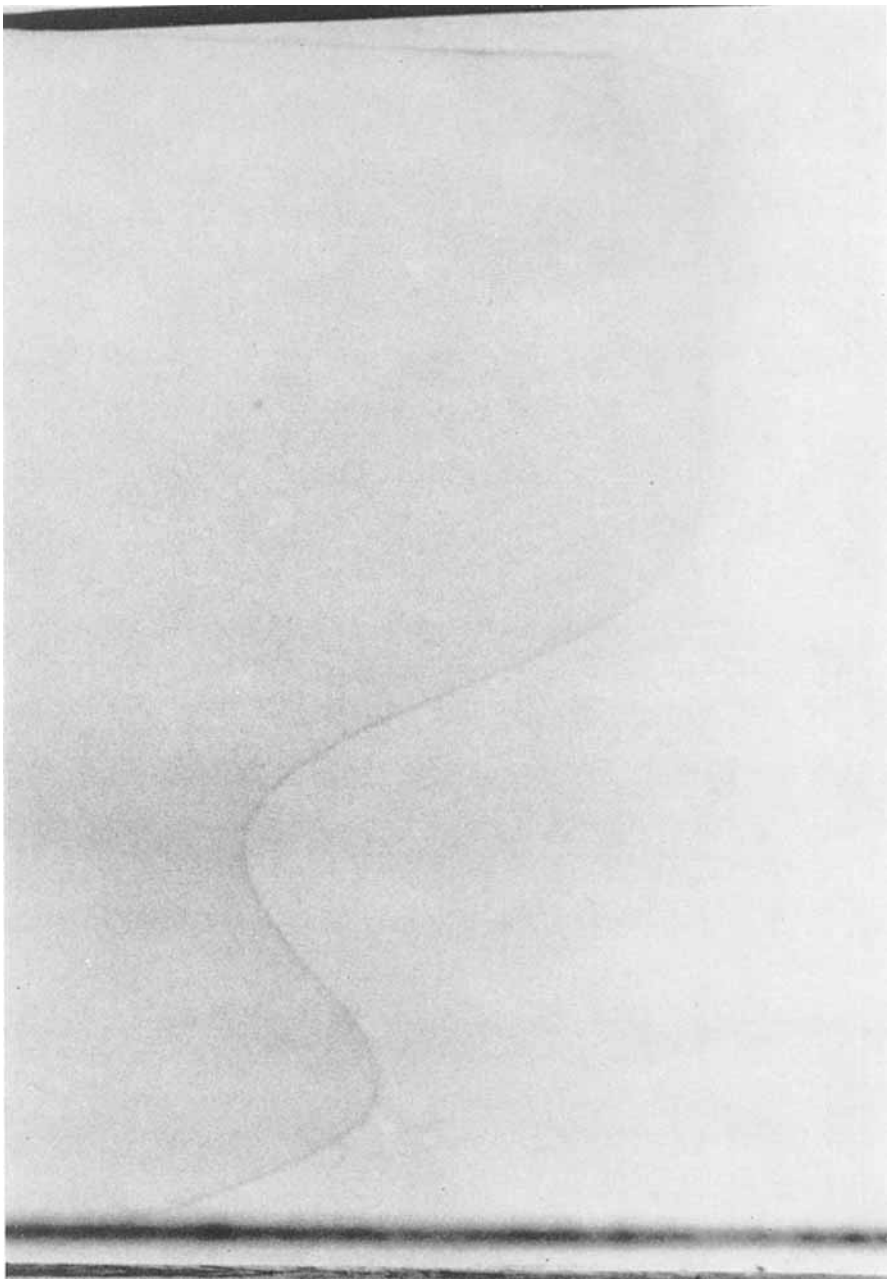

FIGURE 7. Boundary-layer profile with two reversals created by the second-order instability.

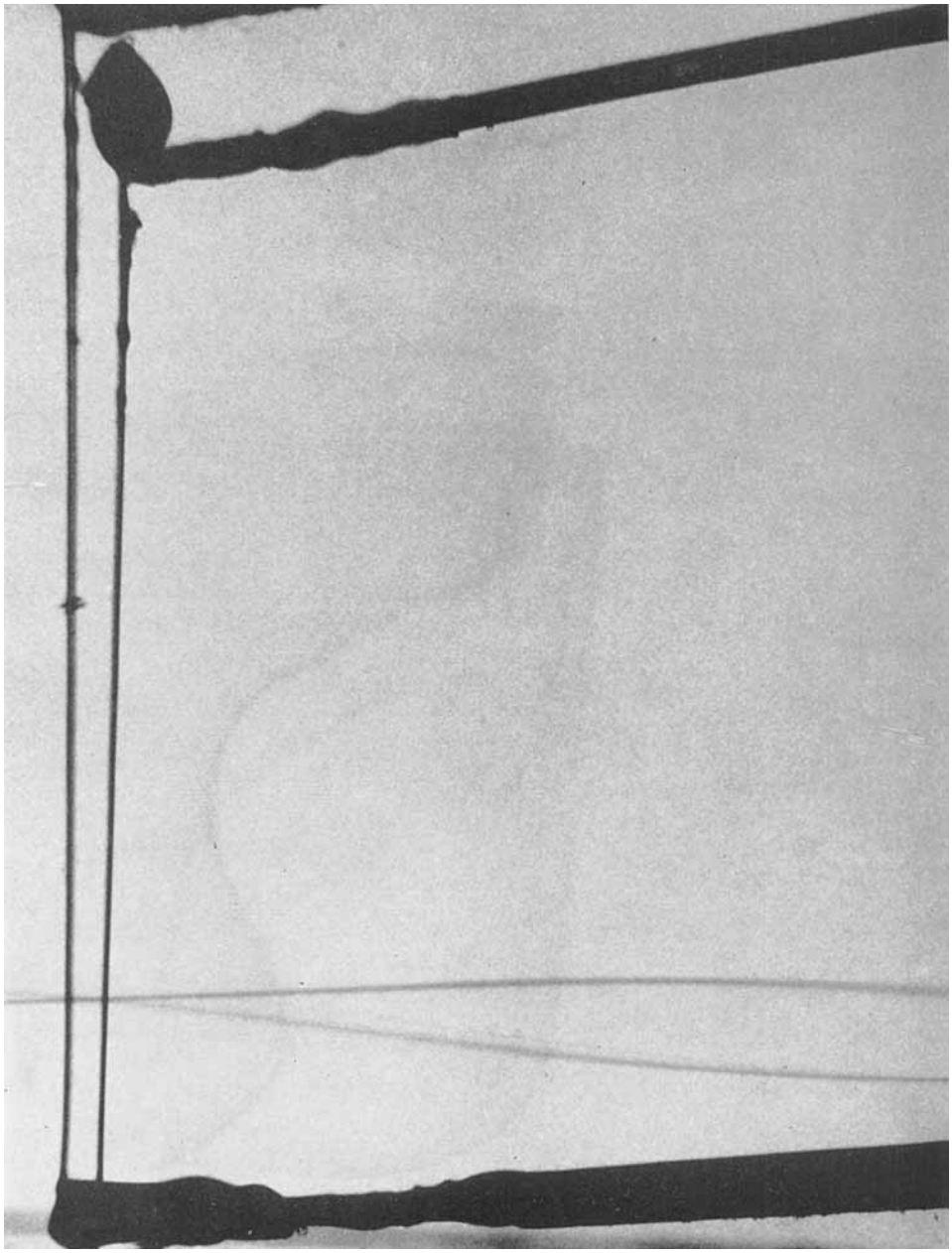

FIGURE 11. Four momentary boundary-layer profiles at $z = 120$ mm and $z = 150$ mm. Two negatives were copied together. The streaklines in the lower part of the picture show that the photographs were taken in the extreme phase positions.